Biosensors and Bioelectronics 222 (2023) 114939

Contents lists available at ScienceDirect

Biosensors and Bioelectronics

journal homepage: www.elsevier.com/locate/bios

Harnessing enhanced CRISPR/Cas12a trans-cleavage activity with extended reporters and reductants for early diagnosis of *Helicobacter pylori*, the causative agent of peptic ulcers and stomach cancer

Jean de Dieu Habimana [a,b], Omar Mukama [a,b,g], Guiquan Chen [c], Mengjun Chen [c], Obed Boadi Amissah [a,b], Lin Wang [a,f], Yujie Liu [a], Yirong Sun [a], Amy L. Li [a], Sihao Deng [d], Jufang Huang [d], Xiao-xin Yan [d], Theobard Rutaganda [e], Dieudonne Mutangana [g], Lin-Ping Wu [a], Rongqi Huang [a,b,j,*], Zhiyuan Li [a,b,d,f,h,i,j,**]

[a] *CAS Key Laboratory of Regenerative Biology, Guangdong Provincial Key Laboratory of Stem Cell and Regenerative Medicine, Guangzhou Institutes of Biomedicine and Health, Chinese Academy of Sciences, Guangzhou, 510530, China*
[b] *University of Chinese Academy of Sciences, 19 Yuquan Road, Shijingshan District, Beijing, 100049, China*
[c] *Department of Gastroenterology, Affiliated Dongguan Hospital, Southern Medical University-Dongguan People's Hospital, Dongguan, 523059, China*
[d] *Department of Anatomy and Neurobiology, Xiangya School of Medicine, Central South University, Changsha, China*
[e] *College of Science 205 Mugar Life Sciences, Northeastern University, 360 Huntington Avenue Boston, MA, 02115, USA*
[f] *Division of Life Sciences and Medicine, University of Science and Technology of China, Hefei, 230026, China*
[g] *Department of Biology, College of Science and Technology, University of Rwanda, Avenue de l'armée, Kigali, P.O. Box: 3900, Rwanda*
[h] *GZMU-GIBH Joint School of Life Sciences, Guangzhou Medical University, Guangzhou, China*
[i] *GIBH-HKU Guangdong-HongKong Stem Cell and Regenerative Medicine Research Centre, GIBH-CUHK Joint Research Laboratory on Stem Cell and Regenerative Medicine, Guangzhou, China*
[j] *Guangzhou Qiyuan Biomedical Co., Ltd, Guangzhou, China*

ARTICLE INFO

Keywords:
Enhanced LbCas12a
Extended reporters
Reductants
Colorimetric readout
Fluorescence readout
Helicobacter pylori

ABSTRACT

Developing rapid and non-invasive diagnostics for *Helicobacter pylori* (HP) is imperative to prevent associated diseases such as stomach gastritis, ulcers, and cancers. Owing to HP strain heterogeneity, not all HP-infected individuals incur side effects. Cytotoxin-associated gene A (CagA), and vacuolating cytotoxin A (VacA) genes predominantly drive HP pathogenicity. Therefore, diagnosing CagA and VacA genotypes could alert active infection and decide suitable therapeutics. We report an enhanced LbCas12a *trans*-cleavage activity with extended reporters and reductants (CEXTRAR) for early detection of HP. We demonstrate that extended ssDNA reporter acts as an excellent signal amplifier, making it a potential alternative substrate for LbCas12a collateral activity. Through a systematic investigation of various buffer components, we demonstrate that reductants improve LbCas12a *trans*-cleavage activity. Overall, our novel reporter and optimal buffer increased the *trans*-cleavage activity to an order of 16-fold, achieving picomolar sensitivity (171 pM) without target pre-amplification. Integrated with loop-mediated isothermal amplification (LAMP), CEXTRAR successfully attained attomolar sensitivity for HP detection using real-time fluorescence (43 and 96 aM), in-tube fluorescence readouts (430 and 960 aM), and lateral flow (4.3 and 9.6 aM) for CagA and VacA, respectively. We also demonstrate a rapid 2-min Triton X-100 lysis for clinical sample analysis, which could provide clinicians with actionable information for rapid diagnosis. CEXTRAR could potentially spot the ^{13}C urea breath test false-negatives. For the first time, our study unveils an experimental outlook to manipulate reporters and reconsider precise cysteine substitution via protein engineering for Cas variants with enhanced catalytic activities for use in diagnostics and genetic engineering.

* Corresponding author. CAS Key Laboratory of Regenerative Biology, Guangdong Provincial Key Laboratory of Stem Cell and Regenerative Medicine, Guangzhou Institutes of Biomedicine and Health, Chinese Academy of Sciences, Guangzhou, 510530, China.
** Corresponding author. CAS Key Laboratory of Regenerative Biology, Guangdong Provincial Key Laboratory of Stem Cell and Regenerative Medicine, Guangzhou Institutes of Biomedicine and Health, Chinese Academy of Sciences, Guangzhou, 510530, China.
E-mail addresses: huang_rongqi@gibh.ac.cn (R. Huang), li_zhiyuan@gibh.ac.cn (Z. Li).

https://doi.org/10.1016/j.bios.2022.114939
Received 7 September 2022; Received in revised form 15 November 2022; Accepted 18 November 2022
Available online 20 November 2022

1. Introduction

Helicobacter pylori (HP) is a Gram-negative pathogen associated with gastritis, duodenal ulcer, and stomach cancer (Chmiela et al., 2017). Cancer is one of the deadliest illnesses, ranking second in worldwide fatalities (Hossen et al., 2019; Khan et al., 2022), and the International Agency for Research on Cancer (IARC) has categorized HP as a group I carcinogen to humans (Kumar et al., 2020). Nearly half of the population in developed countries is infected (Wang et al., 2021), and in certain developing countries, the infection rate is greater than 90% (Chen et al., 2019).

Several virulence factors induce HP pathogenicity; however, CagA and VacA are primarily more virulent (Saxena et al., 2021). These virulence factors interact with gastric epithelial cells, causing inflammation, mucosal degradation, and ultimately gastric cancerogenesis (Ansari and Yamaoka, 2020; Watari et al., 2014). However, not all HP-infected people develop symptoms due to strain heterogeneity. For example, VacA gene is found in all HP strains, but approximately 60% and 50% of HP isolates actively express CagA and VacA cytotoxins, respectively (Maeda et al., 1998; Momtaz et al., 2012). Moreover, based on their virulence factor profiles, strain like HP B38 lacks the Cag-pathogenicity island and exhibits less pro-inflammation (Floch et al., 2017). Therefore, detection of both CagA and VacA could be critical.

Conventional HP diagnostics include invasive biopsy-based tests like endoscopy, histology, culture, rapid urea test (RUT), and sometimes PCR, and non-invasive UBT and serological tests (Alihosseini et al., 2020; Azad et al., 2022). Endoscopy and histology are characterized by poor specificity and uncomfortable endoscopy sampling. RUT and culture are specific but tedious. Besides, several molecular techniques, including PCR, target virulence and non-virulence-associated genes such as cagA, vacA, DupA, OipA, 23 S rRNA, 16 S rRNA, ureA, ureB, ureC, glmM, and hsp60 (Alihosseini et al., 2020; Azad et al., 2022; Saxena et al., 2021). PCR is expensive and unsuitable for on-site testing (Mukama et al., 2020a). Serology tests cannot differentiate between current and past infections or strain heterogeneity (Song et al., 2021). UBT uses the same principle as RUT, but the results require a costly spectrometer, and are not always reliable due to other gastrointestinal tract ureolytic bacteria (Alihosseini et al., 2020). UBT also requires a 4- to 8-week delay to confirm eradication, and it is not recommended for children or pregnant women due to radiation exposure (Alihosseini et al., 2020; Azad et al., 2022). Therefore, there is still a need to advance analytical performance.

CRISPR and its associated Cas proteins have emerged as powerful gene editing and diagnostic tools (Anik et al., 2021; Habimana et al., 2022; Mahmud et al., 2022). CRISPR-based diagnostics (CRISPR-Dx) such as Cas12 and Cas13 proteins exhibit indiscriminate *trans*-cleavage activity on ssDNA or ssRNA (hereafter referred as reporter), respectively. The labelling of the reporter with fluorophores and quenchers generates fluorescence in response to the target presence. This has resulted in the establishment of the first pioneer CRISPR-Dx, such as SHERLOCK (Gootenberg et al., 2017), DETECTR (Chen et al., 2018), and HOLMES (Li et al., 2018) with robust sensitivity and specificity.

More specifically, various CRISPR/Cas12-based diagnostics harnessed the conventional reporter (ConR), TTATT, due to its ability to produce detectable *trans*-cleavage signals. This reporter sequence has evolved into a standard reporter for several CRISPR/Cas12-based fluorescence (Chen et al., 2018; Peng et al., 2020; Shi et al., 2021; Sun et al., 2020; Xiong et al., 2019; Zhang et al., 2020), lateral flow (Nguyen et al., 2020; Wang et al., 2020a; Xiong et al., 2020), and visual in-tube colorimetric readouts (Ding et al., 2020; Wang et al., 2019, 2020b; Wu et al., 2020). However, some groups harnessed various reporter-modified nanoparticles to extend the scope of CRISPR-Dx (Cao et al., 2021; Liang et al., 2022; Zhang et al., 2021). Nguyen et al. (2020) also altered ConR with different nucleotide compositions (TA and GC-rich) while leaving the ConR length constant, and discovered that a TA-rich reporter displayed greater sensitivity. Recently, Liu's group has also reported two novel reporters (NovR), G quadruplex (Li et al., 2020) and G triplex (Li et al., 2021a) with improved signal amplification over the ConR. Also, our group developed a novel reporter for nucleic acid detection in lateral flow biosensors (Mukama et al., 2020c). Despite these advances, there is still a remarkable gap in signal reporters to discern Cas12 substrates preference, which serve as the key signal amplification components of the CRISPR/Cas12 system. In this study, we demonstrate that extending ConR could result in NovR with improved signals that can identify and discriminate weak signals from background noise, reducing false positives, shortening turnaround time, and enhancing the sensitivity.

Besides, several studies on LbCas12a collateral activity utilized various buffer systems (Ding et al., 2020; Nguyen et al., 2020; Wang et al., 2020a; Xiong et al., 2019; Yi et al., 2022; Zhang et al., 2020), but none explored each buffer component's influence. Some studies discussed the effect of metal cations (Li et al., 2021a; Nguyen et al., 2020; Sun et al., 2020). A recent study also reported that bovine serum albumin and L-proline increase the *trans*-cleavage activity of Cas12a (Li et al., 2021b). However, the disparity in the *trans*-cleavage rate between various buffer components remains elusive. A plethora of interactions sustain the native structures of several proteins and peptides, regulating their conformation, folding, and flexibility (Feige et al., 2018). Since, Cas12a possesses 9 cysteine residues (Stella et al., 2018), we reasoned that reducing disulfide bonds with reductants could increase the access of ssDNA substrates in the RuvC catalytic pocket. By properly fine-tuning the buffer recipe, we demonstrate the effect of reducing agents in enhancing LbCas12a *trans*-cleavage activity.

Moreover, the significance of using CRISPR-Dx in biomedical applications is a driving force in advancing these technologies (Habimana et al., 2022; Hossain et al., 2021). We also integrated our CRISPR-Dx with Triton X-100 extraction-free technique (2 min-extraction) to enable streamlined detection. Overall, our work fine-tuned the reporter, buffer, and advanced non-invasive HP diagnosis utilizing real-time fluorescence, lateral flow, and in-tube fluorescence readouts with a quick DNA lysis, and could be adapted to diagnose other infections.

2. Materials and methods

2.1. Materials

Sangon Biotech (Guangzhou, China) supplied recombinant plasmids-containing CagA and VacA genes, and other oligonucleotides (Tables S1–S4). Bst 2.0 DNA polymerase, dNTPs, LbCas12a, and NEBuffers were purchased from NEB (New England, USA). Streptavidin (SA), tetrachloroauric (III) acid ($HAuCl_4aq$), trisodium citrate, and bovine serum albumin (BSA) were purchased from Sigma–Aldrich (Shanghai, China), fiberglass, nitrocellulose membrane (NC), and absorbent papers were from Millipore (Billerica, MA). The XYZ Platform Dispenser HM3030 used for strip design was purchased from Shanghai Kinbio (Shanghai, China). The portable Dhelix-Q5 isothermal fluorescence PCR machine (hereafter referred to as Q5) was purchased from Guangzhou international biological island (Guangzhou, China).

2.2. crRNA design, primer selection, and LAMP assay

The specific crRNAs and LAMP primers for CagA and VacA genes (Table S1) were designed using Benchling and Premier Biosoft databases, respectively. All crRNAs (Table S2) and LAMP primers (Table S3) were confirmed for specificity using NCBI-BLAST. The LAMP reaction was carried out following NEB protocol. Each reaction tube comprised 25 μL of target sample (2 μL), 10 × of isothermal amplification buffer (2.5 μL), 1.4 mM dNTPs, 6 mM MgSO4, 8 U/L Bst DNA polymerase, F3/B3 (0.2 μM), FIB/FIP (1.6 μM), and Loop F/LoopB (0.4 μM) and water. The tubes were incubated at 65 °C for 10 min in a heat block for amplification. The Real-time LAMP was similarly carried out by only

adding SYTO-9. Amplicons were electrophoretically characterized on 2% agarose gel for 50 min at a voltage of 100 V. Unless otherwise noted, all dilutions were done using nuclease-free water, and each reaction contained negative controls.

2.3. LbCas12a-mediated real-time, lateral flow and in-tube fluorescence cleavage assays

A preliminary CRISPR/Cas12a *trans*-cleavage assay was conducted following our previous protocol with slight modification (Mukama et al., 2020b) with 20 μL premix: 10 μL of 2 × NEBuffer 2.1, 1 μL for each of Cas12a (1.2 μM), various ssDNA-FQ reporters (10 μM) (Table S4), crRNA (1 μM), and $MgSO_4$ (100 mM), and 2 μL of target activator, and water. The mixture was incubated in Q5 at 37 °C for 30 min for real-time *trans*-cleavage monitoring. In-tube *trans*-cleavage activity was monitored using a transilluminator or a UV detector (Tseng Hsiang Life Science Ltd., Taipei, Taiwan). The lateral flow experiment was conducted similarly; however, the ssDNA-FQ reporter was substituted with a biotinylated ssDNA reporter for this test. In a one-pot detection assay, we integrated LAMP with LbCas12a-mediated cleavage assay in the same reaction tube with LAMP and CRISPR/Cas12a reagents placed at the bottom and in the lid of an Eppendorf tube. LAMP pre-amplification step was initiated for 10 min at 65 °C, followed by cooling to 37 °C, and spinning down Cas12a to realize a one-pot assay. All experimental tests were performed in three replicates.

2.4. Investigation of buffer systems

All chemicals used for buffer investigation were purchased from Sigma-Aldrich and Thermo Fisher Scientific (Shanghai, China). Table S5 summarizes the concentrations of the main components and respective formulations of buffers. Commercial NEBuffers were used as reference buffers. Additional investigated buffers were prepared similarly by dissolving chemicals in double distilled water, and the pH was adjusted to 7.9 at 25 °C.

2.5. Urea-polyacrylamide gel electrophoresis analysis

To analyze the CRISPR/Cas12a-mediated *trans*-cleaved products of FAM-labeled reporters, we used a 20% denaturing urea-PAGE containing 8 M urea. Before PAGE, the empty gel was pre-run at 120 V for 30 min to remove excess urea. The CRISPR reaction was terminated by adding 6 × loading buffer, and samples were immediately resolved on a gel at a constant voltage of 100 V for 90 min in 1 × TBE buffer using Mini-PROTEAN Tetra Cell system (Bio-Rad, USA). Gels were visualized using a transilluminator after GeneGreen staining.

2.6. Construction of lateral flow strip and assembly

Gold nanoparticles (AuNPs) and streptavidin-conjugated gold nanoparticles (AuNP–SA) based lateral flow strip (LFS) were prepared following our previous method (Mukama et al., 2020c). To design the readout section, the DNA capture probe and biotinylated rabbit polyclonal anti-IgG antibody solutions were sprayed over the NC using a dispenser machine to make up the test and control lines, respectively. The latter was exposed to UV light for 10 min, subsequently dried overnight, and stored at room temperature under low humidity. Finally, all of the LFS sections were joined together, each overlapping by 2 mm, and the LFS of 4 mm was generated using a LFS cutter.

2.7. Extraction of total genomic DNA from bacteria and clinical samples

For specificity assay, bacteria were cultured in LB media at 37 °C. HP was cultured in HP medium supplemented with sterile defibrous sheep blood and bacteriostatic agent at 36 ± 1 °C for 72 h under anaerobic culture bag, oxygen indicator, and anaerobic gas generator (Hope Bio, Qingdao, China). For the validation of CEXTRAR, we used 54 clinical isolates collected from 18 subjects (6 positives and 12 negatives) which have been authenticated using ^{13}C UBT. All clinical samples have been collected from Dongguan People's Hospital, Guangzhou, China (approval number: KYKT 2022-052).

To extract the spiked HP DNA from artificially contaminated milk, an aliquot of 1 mL of milk was centrifuged for 1 min at 12,000 rpm, the supernatant was discarded, and the pellet was mixed with 0.4% Triton X-100, and directly applied in CEXTRAR. Similarly, to compare the efficiency of Triton X-100 DNA extraction, we used 1 mL of HP-containing samples in a commercial TIANGEN Biotech Extraction Kit (Beijing, China). Stool and saliva samples were similarly treated; however, saliva was treated two times with PBS prior to Triton X-100 lysis and LAMP amplification. Stomach biopsies were collected in saline solution and extracted using TIANGEN kit. The PCR of all 18 patient samples was conducted using stool genomic DNA extraction kit (Solarbio life science, Beijing, China).

2.8. Data processing and statistics

Data processing and statistical analysis were carried out in OriginPro (2021). Unless stated otherwise, all experimental values are presented as mean ± SD of three replicates. For statistical significance analysis, unpaired Student's *t*-test (two-tailed), one-way and two-way analysis of variance (ANOVA) and a two-way ANOVA were used to compare data. Data were considered statistically significant for $p < 0.05$ and n.s = not significant.

3. Results and discussion

3.1. Extended conventional reporter enhances LbCas12a trans-cleavage activity

Several CRISPR/Cas12-based diagnostics use a ssDNA oligonucleotide (TTATT) as a conventional reporter (ConR) due to its ability to massively amplify signals (Chen et al., 2018; Ding et al., 2020; Nguyen et al., 2020; Shi et al., 2021; Xiong et al., 2019, 2020). For efficient fluorescence energy transfer, the fluorescent donor and matching acceptor must be closer (Berney and Danuser, 2003; Yun et al., 2005). We hypothesized that extended ConR could regulate/improve LbCas12a *trans*-cleavage by efficient fluorescence transfer/quenching over a greater distance. To test this, the CagA gene was used after crRNA selection (Fig. S1). We generate custom reporters of various lengths (4 T, 6 T, 8 T, and 10 T) by extending ConR (5′-TTATT-3′); hereafter referred to as 2 T, with thymine bases and labeling both ends with fluorescein (FAM) and tetramethylrhodamine (TAMRA) (Fig. 1a). Interestingly, the *trans*-cleavage assessment showed that the longer the reporter, the higher the fluorescence signal (Fig. 1b), and the faster the turnaround response with 10 T showing a high signal-to-background ratio (Fig. 1b and c). However, there was no further signal enhancement for longer reporters (result not shown) due to the steric hindrance induced by longer fragments within the RuvC catalytic site (van Dongen et al., 2021). Moreover, no significant difference in terms of signal and cost was remarked between 6 T, 8 T, and 10 T, which enabled us to select 10 T for further experiments. The reporter 10 T was 3-fold greater than 2 T and could statistically generate a rapid response in 20 min compared to 30 min for 2 T (Fig. 2c). We confirmed the cleaved products of the reporters using urea-PAGE. As shown in (Fig. 2d), smaller molecular weight products were detected due to efficient *trans*-cleavage. The time-course *trans*-cleavage kinetics of 2 T against 10 T under urea-PAGE analysis further confirmed the strong fluorescence of 10 T within 10 min (Fig. 2e). We also investigated whether mixing reporters in different ratios could dramatically increase LbCas12a *trans*-cleavage rate and assay sensitivity (Fig. 2f). Contrary to our hypothesis, the *trans*-cleavage activity decreased in reporter-containing mixtures, presumably due to RuvC domain saturation with excess of substrates (van Dongen et al.,

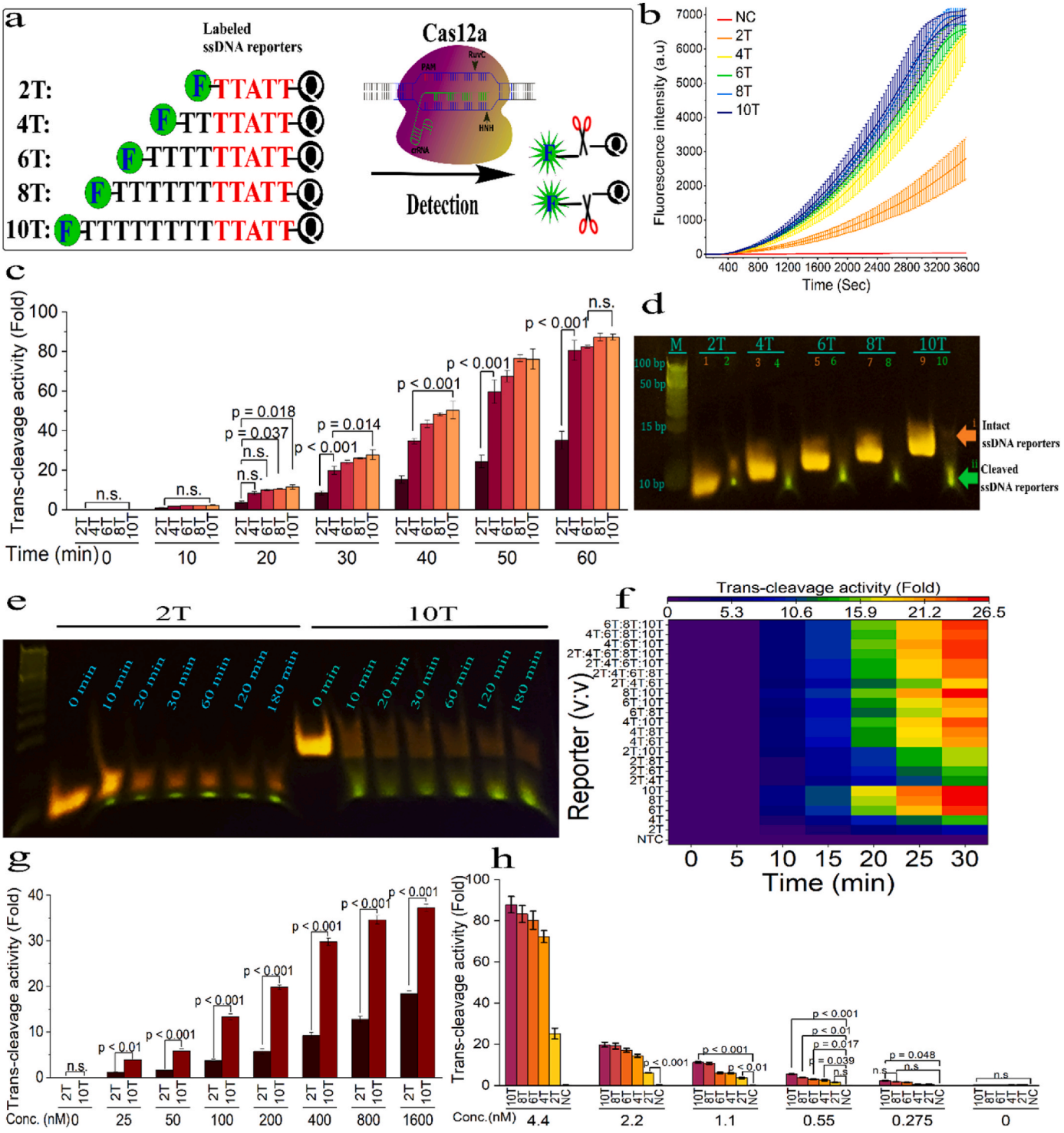

Fig. 1. Extended reporters enhance LbCas12a *trans*-cleavage, signal-to-background ratio, turnaround time, and sensitivity. (a) The ConR (TTATT) was 5′-extended with poly-thymines (2 T, 4 T, 6 T, 8 T, and 10 T), labeled with FAM and TAMRA, and subjected to LbCas12a reaction. (b) The *trans*-cleavage signal increased in reporter length-dependent manner. (c) The *trans*-cleavage and signal-to-background are reporter length and reaction time dependent. (d–e) Urea-PAGE analysis of *trans*-cleaved reporters (d) and time-course (e). The bands (1, 3, 5, 7, 9) and (2, 4, 6, 8, 10) represent LbCas12a reaction before (intact reporters/orange arrow(i)) and after (cleaved reporters/green arrow(ii)) reporter *trans*-cleavage. (f) Synergistic effect of reporter mixtures. (g) Reporter concentrations optimization. (h) Sensitivity assessment and comparison between reporters (2 T, 4 T, 6 T, 8 T, and 10 T) in NEBuffer 2.1.

2021). However, 10 T-containing reporter mixtures exhibited enhanced fluorescence. Moreover, 10 T retained excellent signal under sole-use conditions, also confirming its stand-alone *trans*-cleavage efficiency (Fig. 2f). We further compared 2 T and 10 T at various concentrations, of which at 400 nM, 10 T demonstrated a considerable signal-to-noise ratio, and the fluorescence intensity of 10 T appeared to rise 3.2-fold (Fig. 2g). Furthermore, 10 T showed by significant fluorescence signal, fast turnaround time, sensitivity (Fig. 2h), and could differentiate the concentration of 0.275 nM from the negative control (NC) against 1.1 nM of 2 T.

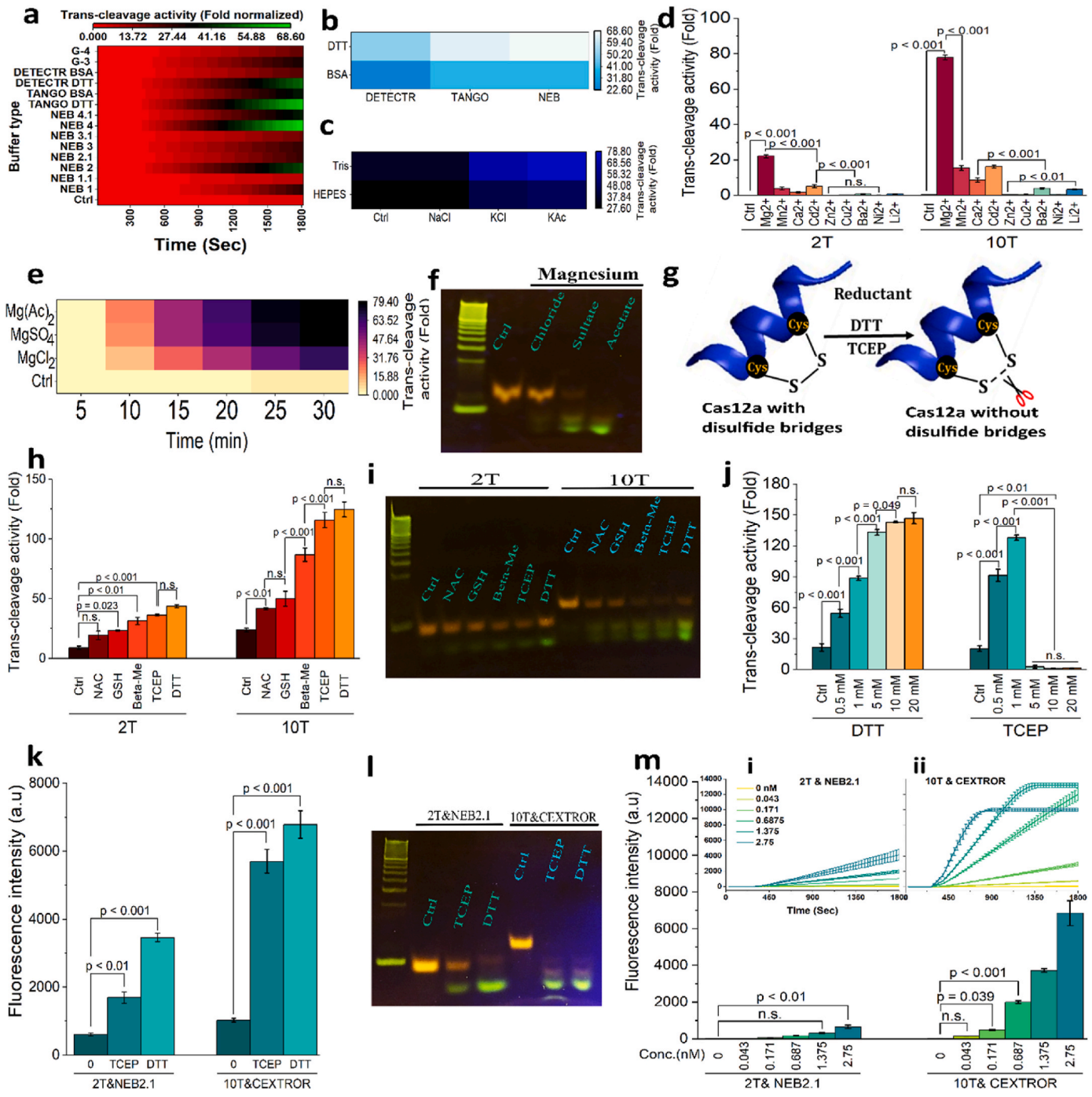

Fig. 2. Optimization of buffer components. (a) Buffer selection. (b) Comparison of NEBuffer, TANGO, and DETECTR buffers supplemented with BSA or DTT. (c) Comparison of buffer components (Tris-HCl and HEPES) in the presence of NaCl, KCl, and K Acetate. (d) Effect of various metal cations on LbCas12a *trans*-cleavage. (e and f) Effect of various salts-containing magnesium. (g, h, and i) Effect of reductants (N-acetylcysteine, NAC; glutathione, GSH; 2-Mercaptoethanol, beta-Mercaptoethanol, beta-Me, DTT, Dithiothreitol; and TCEP, Tris Carboxy Ethyl Phosphene) on the *trans*-cleavage. (j) Effect and comparison of DTT and TCEP under various concentrations. (k and l) Effect of additives (TCEP and DTT) in NEBuffer 2.1 under real-time fluorescence monitoring (k) and denaturing PAGE (l). (m) Comparison of 2 T & NEBuffer 2.1 and 10 T & optimal CEXTRAR buffer under various concentrations. Insets (i and ii) represent the real-time fluorescence analysis of the *trans*-cleavage in 2 T & NEBuffer 2.1 (i) and 10 T & CEXTRAR buffer (ii) under the presence of CagA gene various concentration (0, 0.043, 0.171, 0.6875, 1.375, and 2.75 nM).

3.2. Buffer components influence LbCas12a trans-cleavage, turnaround time, and sensitivity

Buffer components largely determine the spontaneous formation of a higher-level structure essential for protein function. We hypothesized that one of the LbCas12a reaction buffer components might increase the *trans*-cleavage rate, sensitivity, and response time. In our previous experiments (Fig. 1), LbCas12a *trans*-cleavage was conducted using NEBuffer 2.1 (Table S5), a companion buffer of the commercial LbCas12a. We supposed that NEBuffer 2.1, particularly used in several studies (Nguyen et al., 2020; Wang et al., 2019; Wu et al., 2020), might be a sub-optimal buffer. Therefore, we alternatively tested other buffer systems (Table S5, Fig. 2a), and figured out that most NEBuffers, especially NEBuffer 4, exhibited improved LbCas12a *trans*-cleavage kinetics

compared to TANGO and DETECTR buffers (Fig. 2b). We also figured out that Tris-containing recipe exhibited enhanced *trans*-cleavage rate than HEPES recipe at the same pH 7.9 ± 0.02 (Fig. 2c). Similarly, acetate salts showed enhanced *trans*-cleavage than chloride salts (Fig. 2c). That is, potassium acetate demonstrated 2 and 1.5 times higher *trans*-cleavage and a fast response than NaCl and KCl, respectively. We additionally investigated cationic influence. The Mn^{2+}, Ca^{2+}, and Cd^{2+} improved the *trans*-cleavage; however, with reduced kinetics than Mg^{2+} (Fig. 2d). Besides, $MgCl_2$ opted in several studies (Chen et al., 2018; Nguyen et al., 2020; van Dongen et al., 2021; Yuan et al., 2020), exhibited reduced *trans*-cleavage more than acetates and sulfates (Fig. 2e and f).

Many interactions stabilize the native structures of several proteins, determining their conformation, folding, and flexibility (Feige et al., 2018). The disulfide bond between two cysteine residues in a protein is one type of such interaction (Kuan et al., 2016) (Fig. 2g, Fig. S2). Further assessments also revealed that DTT-containing buffers markedly improved LbCas12a *trans*-cleavage compared to BSA-containing buffers (Fig. 2b), attributable to disulfide bond reduction (Frändberg et al., 2001). Similar activity was observed in other reductants, particularly TCEP-containing buffer (Fig. 2h and i), and *trans*-cleavage activity was concentration-dependent (Fig. 2j), with TCEP concentrations greater than 2 mM inhibiting *trans*-cleavage (Fig. S3a). This could be because further degradation of buried disulfide bonds generally results in the loss of a protein's native conformation (Feige et al., 2018). Although DTT activity increased at higher concentration ranges over TCEP, TCEP showed excellent stability at 25 ± 2 °C (Fig. S3b). Besides, to confirm the effect of TCEP and DTT, we investigated whether the two reductants could be added to NEBuffer 2.1 to improve its efficiency. Interestingly, we observed an enhanced *trans*-cleavage activity in TCEP- and DTT-containing NEBuffer 2.1 (Fig. 2k and l).

Furthermore, we optimized each buffer component to assess their impact on LbCas12a (Fig. S4 a, b, and c). The final optimized buffer, named CEXTRAR buffer (Table S5) was 4-fold higher than NEBuffer 2.1 (Fig. S4d). With CEXTRAR buffer, LbCas12a activity peaked in the range of physiological pH, but not in acidic pH (Fig. S5). This activity was achieved when 4 × CEXTRAR buffer was used (Fig. S6). Excellent CEXTRAR buffer sensitivity (171 pM) was confirmed with 10 T reporter, while 2750 pM was achieved when buffer NEBuffer 2.1 and 2 T reporter were used (Fig. 2 m, insets, i and ii), with 16-fold sensitivity enhancement.

3.3. LAMP improves the sensitivity and specificity of CEXTRAR for real-time fluorescence, lateral flow, and in-tube colorimetric detection of HP

While CEXTRAR could detect as low as 171 pM without an additional step of amplification, we increased sensitivity by using CEXTRAR in combination with LAMP pre-amplification in a one-pot reaction. Initially, we evaluated the sensitivity of CEXTRAR using the Q5 machine. After primer selection (Fig. S7 a, b, and c) and response time optimizations (Fig. S7 d, e, and f), we performed LAMP using serially diluted concentrations of target genes. The LAMP pre-amplification improved CEXTRAR sensitivity down to 43 aM (51 copies/μL) and 96 aM (115 copies/μL) for CagA and VacA, respectively (Fig. 3 a, b).

Besides, we leveraged the system into on-site diagnostics by designing a custom capture probe that directly hybridizes a ssDNA reporter at the test band to transduce the CRISPR/Cas12a signal without auxiliary carriers (Fig. S8). For our previous approach (Mukama et al., 2020c), two bands represent a negative test, while one band confirms a positive infection. Interestingly, the approach achieved as low as 1.8 copies in clinical samples; however, with a long incubation period (45

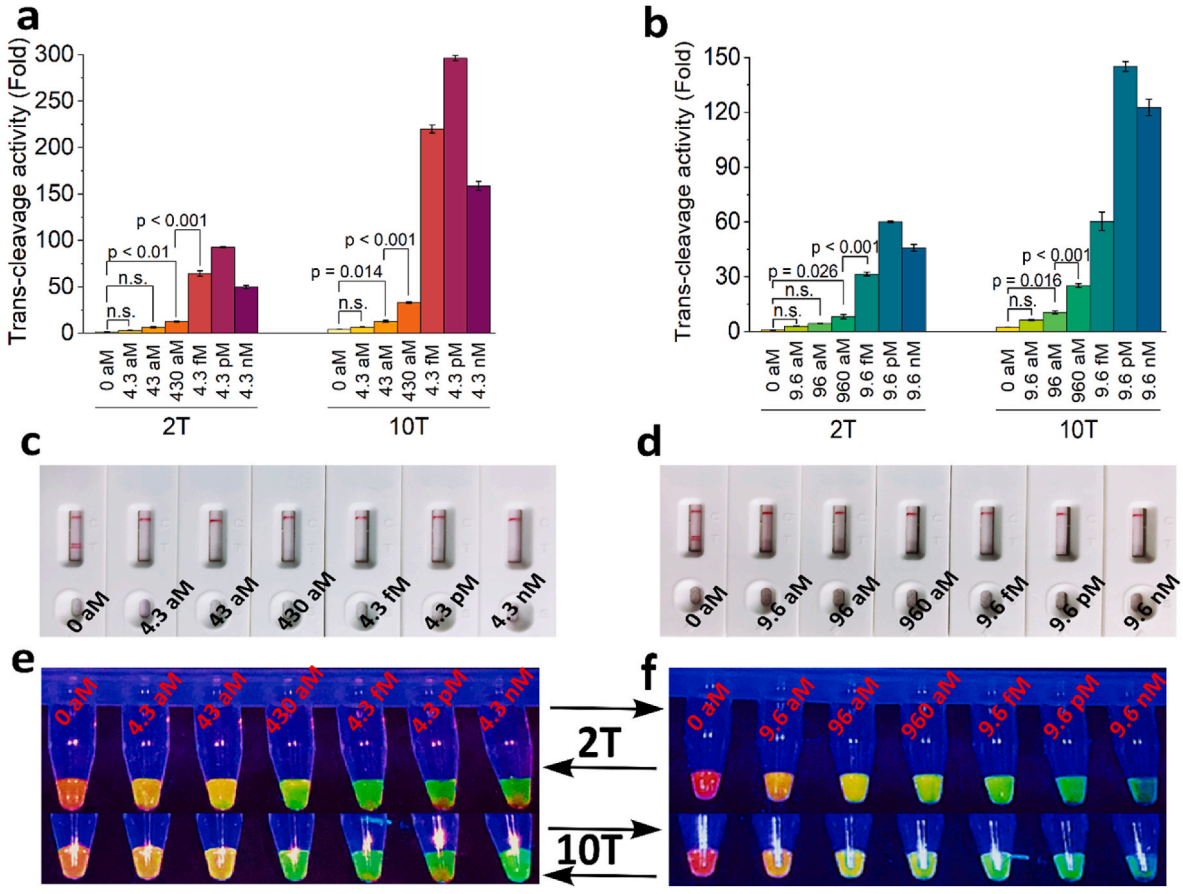

Fig. 3. LAMP improves the sensitivity of CEXTRAR. CEXTRAR sensitivity for CagA gene (a, c, and e) and VacA gene (b, d, and f). Sensitivity of real-time fluorescence monitoring (a, b), lateral flow assay (c, d, only the results of 10 T have been shown), and in-tube fluorescence detection (e, f).

min) for Cas12a-mediated assay and a lateral flow strip readout (5 min). We suspected that a suboptimal buffer was to blame for the slow kinetics (DETECTR-BSA, Table S5). Therefore, we used CEXTRAR buffer (Fig. S9), which successfully reduced the incubation time from 45 to 20 min (Table S5), resulting in enhanced test lines in less than 2 min (Fig. S9). The sensitivity of LFB was then investigated using CEXTRAR-optimized conditions. We confirmed a 10-fold sensitivity increase (4.3 and 9.6 aM) over the real-time fluorometer, with greatly enhanced test bands (Fig. 3 c and d).

Besides, tube opening increases cross-contamination. Therefore, we established a one-pot detection assay by combining LAMP and CRISPR reagents, which were placed at the bottom and inside of the tube lid, respectively. LAMP reaction was conducted for 10 min before applying spinning to initiate CRISPR reaction. Within less than 1 h, we detected as low as 430 aM and 960 aM using CagA and VacA HP plasmids, respectively (Fig. 3 e and f). Thus, a one-pot in-tube fluorescence readout does not only prevent aerosol contamination, but also simplifies reaction processing, reduces hands-on-sample, and promises massive scalability.

Furthermore, we assessed the specificity of CEXTRAR using several pathogens that can simultaneously co-exist in the same clinical sample. As shown in (Fig. 4a and b, c, d, e, and f), 8 infectious pathogens were applied to CEXTRAR, which demonstrated excellent specificity, depicting that all LAMP primers and crRNAs successfully genotyped all tested pathogens with no cross-reactivity. Moreover, we generated point mutations in the DNA target to assess the effect of mismatch on the *trans*-cleavage in CEXTRAR assay (Fig. 4g). In accordance with previous studies (Chen et al., 2018; Nguyen et al., 2020), we realized that mutations in the PAM proximal nucleotides remarkably reduce the *trans*--cleavage (Fig. 4h, Fig. S10). The same effect was also observed in multiple (two or three mismatches) point mutations (Fig. 4h, Fig. S10).

3.4. Clinical sample analysis using fast genomic DNA extraction-free approach

To reduce the assay time, hands-on sample, and DNA extraction complexity, specimen processing is still limiting CRISPR-Dx. Therefore, we investigated previously reported DNA extraction strategies (Arizti--Sanz et al., 2020; Mukama et al., 2020b; Myhrvold et al., 2018) in order to integrate CEXTRAR with a straightforward extraction protocol (Fig. 5a and S10 a). We tested commercial lysis buffers, chemicals, and heat treatments on HP cells. Heat (95 °C for 5 min) or chemicals alone reduced DNA yields in several scenarios (Fig. S11 b). Intriguingly, a non-ionic detergent, Triton X-100 (0.4%), and an initial centrifugation step at 12,000 rpm for 1 min increased DNA yields more than several heat and chemical treatments (Fig. S11 b). Triton X-100 yielded twice as much DNA as a TIANGEN Biotech extraction kit (Fig. S11 c). A reduced

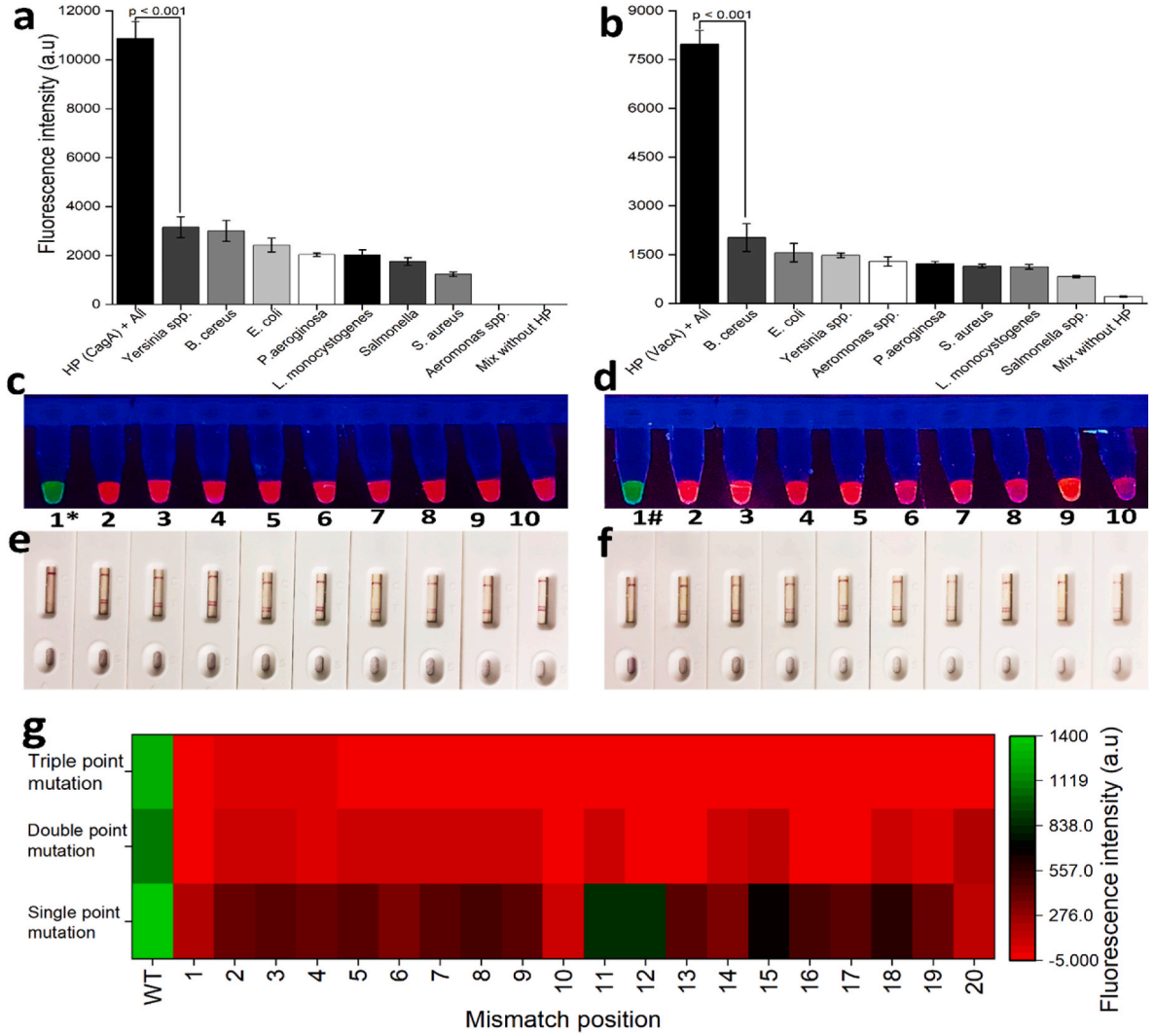

Fig. 4. Assessment of CEXTRAR specificity for CagA gene (a, c, and e) and VacA gene (b, d, and f). The specificity for columns of HP (CagA and VacA) was assessed under the presence of all pathogens, whereas the column for "Mix" represents all pathogens mixed together excluding HP. Specificity assessment using VacA mutated gene with single (S1-20), double (D1-20), and triple point mutations (S1-20) (g).

DNA output from TIANGEN kit could be attributed to several repeated purification steps using various buffers. Our results are consistent with previous studies that CRISPR/Cas systems tolerate high impurities (Myhrvold et al., 2018; Pardee et al., 2016). To validate CEXTRAR for the detection of HP clinical samples, we examined 54 clinical isolates from 18 patients (Table S6), including saliva, stool, and stomach biopsy samples initially authenticated using the ^{13}C UBT. Originally, we tested 10 patients (30 clinical isolates)—and the patients were categorized as follows: UBT-positive patients (P1, P2, P5, P6, P10) and UBT-negative patients (P3, P4, P7, P8, P9). We figured out that saliva and stool but not biopsy samples could be analyzed without an initial step of LAMP amplification (Fig. S12). We also realized that the amount of stool sample reflects the extent of infection (Fig. S13). Confoundingly, although we observed a remarkable activation of LbCas12a in clinical samples using Triton X-100 LAMP amplification to boost the sensitivity, our results did not corroborate with ^{13}C UBT negative samples because all the patients tested positive for CagA and VacA genes (100% sensitivity, 0% specificity) (Fig. S12), (Table S6). Thus, we sought confirmatory methods to determine the inconsistency's cause. We used HP selective media and antibiotics to culture 30 clinical isolates for live HP. We unexpectedly found bacterial growth on all plates except several biopsy samples and negative controls (Fig. S14). The low bacterial load in biopsies reflects a reduced *trans*-cleavage, as shown in (Fig. 5 b and c).

We collected more UBT-negative patient samples to investigate LbCas12a activation in negative samples and determine cut-off values. Triton X-100 direct lysis showed that additional 8 UBT samples—7 negatives (P11, P12, P13, P14, P15, P17, and P18) and one positive (P16)—tested positive for CagA and VacA genes (results not shown). Thus, we integrated CEXTRAR with amplification to improve the specificity through primers. Interestingly, UBT corroborated CEXTRAR-LAMP through CagA gene (66.7% sensitivity and 58.3% specificity), but VacA gene specificity was still dubious (83.3% sensitivity, 16.6% specificity) (Fig. 5). We subsequently used PCR to confirm HP VacA genotype infection in 18 patients. We realized that 15 patient samples showed a 296-bp electrophoretic band (Fig. S15a), consistent with NCBI primer BLAST. Sanger sequencing of the amplicons confirmed that the fragments under electrophoresis matched the vacA gene sequence in GenBank (Fig. S15b). This suggests that CEXTRAR-LAMP can detect false-negatives from ^{13}C UBT. Furthermore, many samples for UBT and CEXTRAR concordance were observed in the HP VacA genotype cluster, implying that all HP strains carry the VacA gene and differ in VacA expression and toxin activity (McClain et al., 2017). Nevertheless, more patients could be admitted for further observational studies on our method's specificity. Due to false negatives, UBT could be less sensitive than CEXTRAR. Several factors could explain the testing discrepancy. The number of bacterial loads present during sampling, the requirement of basal breath sample, the dose of 13C urea capsule ingested, the sampling time since all patients are advised to fast before the UBT test, and the cut-off value could cause UBT false negatives (Gisbert and Pajares, 2005).

Besides, HP can survive in artificially contaminated milk stored at 4 °C for 5–9 days in pasteurized milk and 6–12 days in sterilized milk (Quaglia and Dambrosio, 2018). HP's long-term survival in milk may be due to milk's high urea content and HP's ability to survive at low pH. To this end, we tested CEXTRAR-free amplification for HP detection in milk. Local supermarket sterile fresh milk was purchased, diluted (10%), and spiked with HP cells. The supernatant from Triton X-100 (0.4%) lysis was used. The matrix effect reduced *trans*-cleavage activity in whole milk samples compared to 10% spiked milk samples (Fig. S16). HP-free sterilized milk showed no *trans*-cleavage activity. We also found no discrepancy in specificity when analyzing fresh milk samples, highlighting the need to investigate LbCas12a activation in clinical heterogeneous human samples.

4. Discussion

The UBT, RUT, and PCR have been developed for HP detection; however, they are tedious and sometimes require expensive equipment (Alihosseini et al., 2020; Azad et al., 2022; Saxena et al., 2021). In addition, predominated clinical detection methods rely on UBT and serology, which exhibit poor specificity and inefficiency in eradication diagnosis. Besides, PCR relies on HP genes as promising biomarkers (Sulo and Šipková, 2021), but is also clinically restricted by its cost, tediousness, on-use expertise, expensive extraction kits, and pure samples.

The use of CRISPR/Cas system for the detection of nucleic acids has revolutionized diagnosis by enhancing not only the sensitivity and specificity, but also present simplicity, inexpensiveness, on-site application, and complex sample tolerance (Habimana et al., 2022). However, investigating disparities in Cas12 proteins in *trans*-cleavage of reporter and results readouts is still of great importance. We proposed a sensitive LbCas12a-based method that *trans*-cleaves well-tuned extended reporters to generate highly detectable signals with improved sensitivity, specificity, and quick turnaround time. Buffer optimization accelerated LbCas12a *trans*-cleavage activity and improved more significantly by acetate and DTT/TCEP-containing buffers (Fig. 2). CEXTRAR achieved a 16-fold sensitivity improvement compared to conventional reporters and Cas12a companion buffer (Fig. 2m), and could reach attomolar level when integrated with LAMP in one-pot using real-time fluorescence reporting, lateral flow visualization, and in-tube fluorescence readout. The physico-chemical properties of Cas12a, such as viscosity and stickiness, enable LAMP and CRISPR to occur at 65 and 37 °C, respectively, by creating two separate phases of reagents, establishing a one-pot assay using a simple spinning without sacrificing the sensitivity.

To achieve a deployable diagnostic, we developed CEXTRAR Triton X-100 lysis, enabling minimal clinical sample (saliva and stool) processing and reducing hands-on samples. This promises a high-throughput sample extraction with excellent yield, simplicity, and short time, and avoids invasive detection methods that require stomach biopsies.

5. Conclusions

In summary, we unveil a novel enhanced CRISPR/Cas12a *trans*-cleavage activity with extended reporters and reductants, named CEXTRAR, to detect HP based on potential inflammatory and carcinogenic virulence markers (CagA and VacA genes), enabling early prediction of active infection and high risk of disease evolution. CEXTRAR-LAMP is ultrasensitive (attomolar level), and harnesses Triton X-100 lysis for clinical samples analysis, and has shown to excel ^{13}C UBT due to the potential to discriminate inconclusive tests. Our method holds potential at the POC application due to the versatility of CEXTRAR assay, tunable reporters, and flexibility of end-point result interpretation using real-time fluorescence, in-tube fluorescence or lateral flow readouts. Thus, CEXTRAR could alternatively be customized for other pathogens or genetic diseases detection by only manipulating the LAMP primers and Cas12a crRNAs. In the future, the engineering of cysteine residues can be applied to Cas proteins, resulting in enhanced Cas for use in diagnostics and genetic engineering.

CRediT authorship contribution statement

Jean de Dieu Habimana: Formal analysis, Conceptualization, Data curation, Methodology, Software, Writing – original draft. **Omar Mukama:** Formal analysis, Conceptualization, Data curation, Writing – review & editing. **Guiquan Chen:** Formal analysis, Data curation, Investigation. **Mengjun Chen:** Formal analysis, Investigation, Visualization. **Obed Boadi Amissah:** Data curation, Formal analysis, Software, Writing – review & editing. **Lin Wang:** Data curation, Formal analysis.

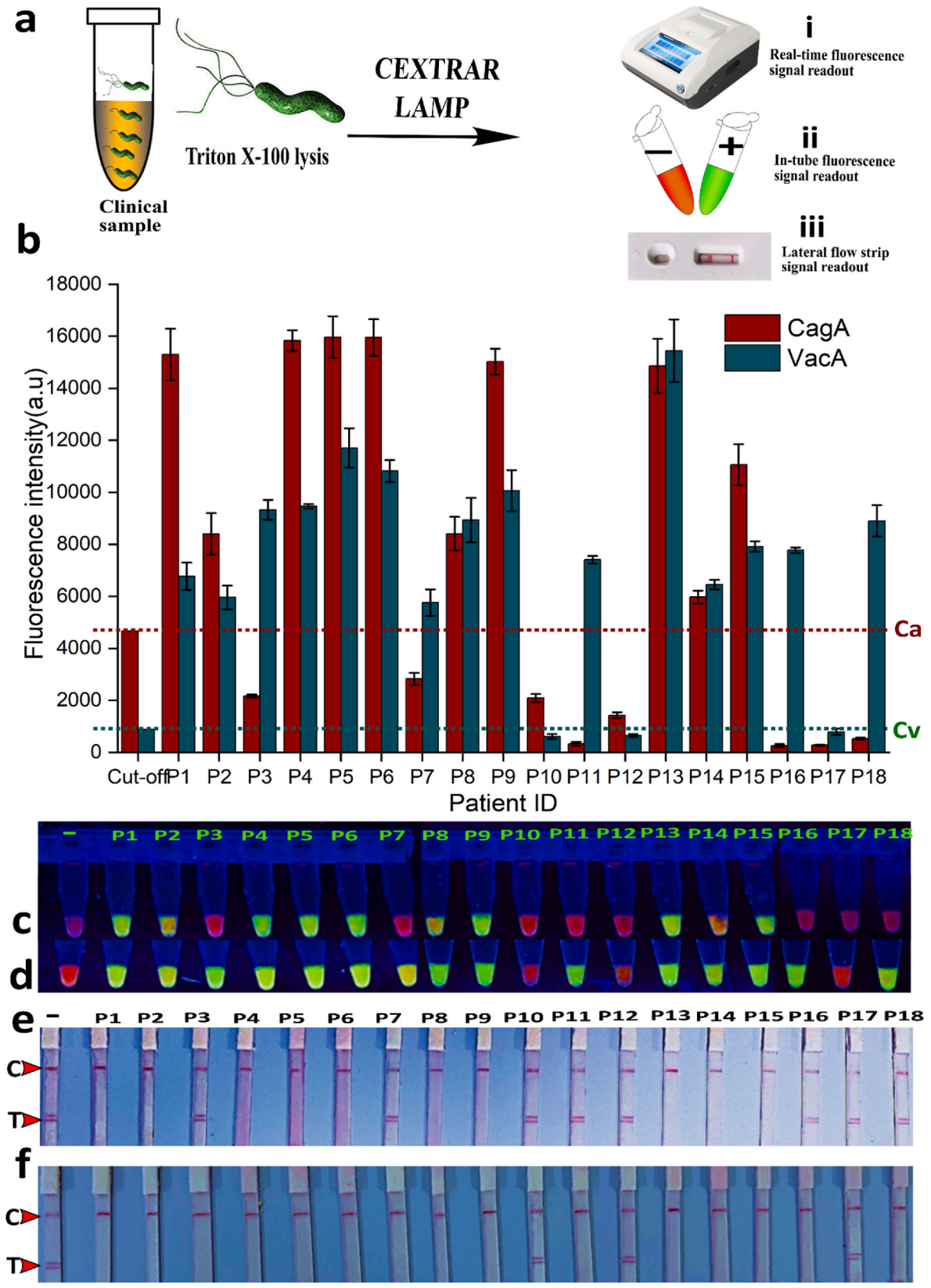

Fig. 5. CEXTRAR-integrated LAMP improves the specificity for the screening and differentiation of HP CagA and VacA genotypes. (a) Saliva sample was treated with Triton X-100, amplified using LAMP, and applied to CEXTRAR. The results could be assessed using three different readouts depending on the user preferences; real-time fluorescence monitoring (i, b), in-tube fluorescence signal readout (ii, c, d), and LFS visualization (iii, e, f). (c and e) represent CagA gene, (d and f) represent VacA gene. Ca and Cv represent the cut-off values for CagA and VacA genes, respectively, calculated based on the three times standard deviation above the negative control. C: control line, T: test line.

Yujie Liu: Data curation, Formal analysis. **Yirong Sun:** Data curation, Formal analysis, Visualization. **Amy L. Li:** Data curation, Formal analysis. **Sihao Deng:** Data curation, Formal analysis. **Jufang Huang:** Data curation, Formal analysis. **Xiao-xin Yan:** Data curation, Formal analysis. **Theobard Rutaganda:** Data curation, Formal analysis. **Dieudonne Mutangana:** Data curation, Formal analysis. **Lin-Ping Wu:** Data curation, Formal analysis. **Rongqi Huang:** Data curation, Formal analysis, Supervision. **Zhiyuan Li:** Formal analysis, Supervision, Conceptualization, Funding acquisition, Project administration, Writing – review & editing.

Declaration of competing interest

The authors declare that they have no known competing financial interests or personal relationships that could have appeared to influence the work reported in this paper.

Data availability

Data will be made available on request.

Acknowledgments

This work was supported by the Stem Cell New Drug, Innovation Hunan Team (2019RS1088), 2020 Hunan Hunan province Key R&D Plan (2020SK2137), Hunan Provincial Natural Science Foundation (2020JJ5698), (2020JJ9047), (2021JJ30800), Guangdong Provincial Natural Science Foundation (2021A1515010526), Changsha City Science & Technology Plan (kq2001031). J.d.D. H. is sponsored by the CAS-TWAS President's Fellowship for international Ph.D students.

Appendix A. Supplementary data

Supplementary data to this article can be found online at https://doi.org/10.1016/j.bios.2022.114939.

References

Alihosseini, S., Jaberinezhad, M., SadeghpourHeravi, F., Ghotaslou, R., Ebrahimzadeh Leylabadlo, H., 2020. Gene Rep 20, 100749.
Anik, M.I., Hossain, M.K., Hossain, I., Mahfuz, A.M.U.B., Rahman, M.T., Ahmed, I., 2021. Nano Select 2, 1146–1186.
Ansari, S., Yamaoka, Y., 2020. Int. J. Mol. Sci. 21, 7430.
Arizti-Sanz, J., Freije, C.A., Stanton, A.C., Petros, B.A., Boehm, C.K., Siddiqui, S., Shaw, B.M., Adams, G., Kosoko-Thoroddsen, T.-S.F., Kemball, M.E., Uwanibe, J.N., Ajogbasile, F.V., Eromon, P.E., Gross, R., Wronka, L., Caviness, K., Hensley, L.E., Bergman, N.H., MacInnis, B.L., Happi, C.T., Lemieux, J.E., Sabeti, P.C., Myhrvold, C., 2020. Nat. Commun. 11, 5921.
Azad, K.N., Realegeno, S.E., Kagan, R.M., Schwab, D.A., Batterman, H.J., Marlowe, E.M., 2022. Clin. Microbiol. Newsl. 44, 51–61.
Berney, C., Danuser, G., 2003. Biophys. J. 84, 3992–4010.
Cao, Y., Wu, J., Pang, B., Zhang, H., Le, X.C., 2021. Chem. Commun. 57, 6871–6874.
Chen, J.S., Ma, E., Harrington, L.B., Da Costa, M., Tian, X., Palefsky, J.M., Doudna, J.A., 2018. Science 360, 436–439.
Chen, L., Li, X., Zou, T., Wang, T., Cui, X., Chen, Y., Zhang, C., Zhao, S., 2019. Analyst 144, 4086–4092.
Chmiela, M., Karwowska, Z., Gonciarz, W., Allushi, B., Stączek, P., 2017. World J. Gastroenterol. 23 (9), 1521–1540.
Ding, X., Yin, K., Li, Z., Lalla, R.V., Ballesteros, E., Sfeir, M.M., Liu, C., 2020. Nat. Commun. 11, 4711.
Feige, M.J., Braakman, I., Hendershot, L.M., 2018. CHAPTER 1.1 disulfide bonds in protein folding and stability. In: Oxidative Folding of Proteins: Basic Principles, Cellular Regulation and Engineering. The Royal Society of Chemistry, pp. 1–33.
Floch, P., Mégraud, F., Lehours, P., 2017. Toxins 9, 132.
Frändberg, P.-A., Doufexis, M., Kapas, S., Chhajlani, V., 2001. Biophys. Res. Commun. 281, 851–857.
Gisbert, J.P., Pajares, J.M., 2005. Dig. Liver Dis. 37, 899–906.
Gootenberg, J.S., Abudayyeh, O.O., Lee, J.W., Essletzbichler, P., Dy, A.J., Joung, J., Verdine, V., Donghia, N., Daringer, N.M., Freije, C.A., 2017. Science 356, 438–442.
Habimana, J.d.D., Huang, R., Muhoza, B., Kalisa, Y.N., Han, X., Deng, W., Li, Z., 2022. Biosens. Bioelectron. 203, 114033.
Hossain, M.K., Khan, M.I., El-Denglawey, A., 2021. Appl. Mater. 24, 101104.
Hossen, S., Hossain, M.K., Basher, M.K., Mia, M.N.H., Rahman, M.T., Uddin, M.J., 2019. J. Adv. Res. 15, 1–18.
Khan, M.I., Hossain, M.I., Hossain, M.K., Rubel, M.H.K., Hossain, K.M., Mahfuz, A.M.U. B., Anik, M.I., 2022. ACS Appl. Bio Mater. 5, 971–1012.
Kuan, S.L., Wang, T., Weil, T., 2016. Chem. Eur J. 22, 17112–17129.
Kumar, S., Metz, D.C., Ellenberg, S., Kaplan, D.E., Goldberg, D.S., 2020. Gastroenterology 158, 527–536 e527.
Li, S.-Y., Cheng, Q.-X., Wang, J.-M., Li, X.-Y., Zhang, Z.-L., Gao, S., Cao, R.-B., Zhao, G.-P., Wang, J., 2018. Cell Discov 4, 20.
Li, T., Hu, R., Xia, J., Xu, Z., Chen, D., Xi, J., Liu, B.-F., Zhu, J., Li, Y., Yang, Y., Liu, M., 2021a. Biosens. Bioelectron. 187, 113292.
Li, Y., Li, T., Liu, B.-F., Hu, R., Zhu, J., He, T., Zhou, X., Li, C., Yang, Y., Liu, M., 2020. Chem. Commun. 56, 12526–12529.
Li, Z., Zhao, W., Ma, S., Li, Z., Yao, Y., Fei, T., 2021b. Biosens. Bioelectron. 192, 113493.
Liang, J., Teng, P., Hu, L., He, G., Song, Q., Zhang, Y., Peng, B., Li, G., Xiao, W., Cao, D., Tang, Y., 2022. Anal. Chim. Acta 1225, 340203.
Maeda, S., Ogura, K., Yoshida, H., Kanai, F., Ikenoue, T., Kato, N., Shiratori, Y., Omata, M., 1998. Gut 42, 338.
Mahmud, N., Anik, M.I., Hossain, M.K., Khan, M.I., Uddin, S., Ashrafuzzaman, M., Rahaman, M.M., 2022. ACS Appl. Bio Mater. 5, 2431–2460.
McClain, M.S., Beckett, A.C., Cover, T.L., 2017. Toxins 9, 316.
Momtaz, H., Souod, N., Dabiri, H., Sarshar, M., 2012. World J. Gastroenterol. 18, 2105–2111.
Mukama, O., de Dieu Habimana, J., Meng, X., Ting, Y., Songwe, F., Al Farga, A., Mugisha, S., Rwibasira, P., Li, Z., Zeng, L., 2020a. Anal. Biochem. 113762.
Mukama, O., Wu, J., Li, Z., Liang, Q., Yi, Z., Lu, X., Liu, Y., Liu, Y., Hussain, M., Makafe, G.G., 2020b. Biosens. Bioelectron., 112143
Mukama, O., Yuan, T., He, Z., Li, Z., Habimana, J.d.D., Hussain, M., Li, W., Yi, Z., Liang, Q., Zeng, L., 2020c. Sensor. Actuator. B Chem. 316, 128119.
Myhrvold, C., Freije, C.A., Gootenberg, J.S., Abudayyeh, O.O., Metsky, H.C., Durbin, A. F., Kellner, M.J., Tan, A.L., Paul, L.M., Parham, L.A., 2018. Science 360, 444–448.
Nguyen, L.T., Smith, B.M., Jain, P.K., 2020. Nat. Commun. 11, 4906.
Pardee, K., Green, A.A., Takahashi, M.K., Braff, D., Lambert, G., Lee, J.W., Ferrante, T., Ma, D., Donghia, N., Fan, M., Daringer, N.M., Bosch, I., Dudley, D.M., O'Connor, D. H., Gehrke, L., Collins, J.J., 2016. Cell 165, 1255–1266.
Peng, S., Tan, Z., Chen, S., Lei, C., Nie, Z., 2020. Chem. Sci. 11, 7362–7368.
Quaglia, N.C., Dambrosio, A., 2018. World J. Gastroenterol. 24, 3472–3487.
Saxena, K., Chauhan, N., Jain, U., 2021. Anal. Biochem. 630, 114325.
Shi, K., Xie, S., Tian, R., Wang, S., Lu, Q., Gao, D., Lei, C., Zhu, H., Nie, Z., 2021. Sci. Adv. 7, 7802.
Song, X., Lv, M.-M., Lv, Q.-Y., Cui, H.-F., Fu, J., Huo, Y.-Y., 2021. Microchem. J. 166, 106243.
Stella, S., Mesa, P., Thomsen, J., Paul, B., Alcón, P., Jensen, S.B., Saligram, B., Moses, M. E., Hatzakis, N.S., Montoya, G., 2018. Cell 175, 1856–1871.
Sulo, P., Šipková, B., 2021. World J. Gastroenterol. 27, 7100–7112.
Sun, Y., Liu, H., Shen, Y., Huang, X., Song, F., Ge, X., Wang, A., Zhang, K., Li, Y., Li, C., Wan, Y., Li, J., 2020. ACS Omega 14814–14821.
van Dongen, J.E., Berendsen, J.T.W., Eijkel, J.C.T., Segerink, L.I., 2021. Biosens. Bioelectron. 194, 113624.
Wang, B., Wang, R., Wang, D., Wu, J., Li, J., Wang, J., Liu, H., Wang, Y., 2019. Anal. Chem. 91, 12156–12161.
Wang, X., Ji, P., Fan, H., Dang, L., Wan, W., Liu, S., Li, Y., Yu, W., Li, X., Ma, X., Ma, X., Zhao, Q., Huang, X., Liao, M., 2020a. Commun. Biol. 3, 62.
Wang, X., Zhong, M., Liu, Y., Ma, P., Dang, L., Meng, Q., Wan, W., Ma, X., Liu, J., Yang, G., Yang, Z., Huang, X., Liu, M., 2020b. Sci. Bull. 65, 1436–1439.
Wang, Z., Wang, H., Cheng, X., Geng, J., Wang, L., Dong, Q., Liu, C., Chi, Z., Chi, Z., 2021. Biosens. Bioelectron. 193, 113551.
Watari, J., Chen, N., Amenta, P.S., Fukui, H., Oshima, T., Tomita, T., Miwa, H., Lim, K.-J., Das, K.M., 2014. World J. Gastroenterol. 20, 5461–5473.
Wu, H., He, J.-s., Zhang, F., Ping, J., Wu, J., 2020. Anal. Chim. Acta 1096, 130–137.
Xiong, D., Dai, W., Gong, J., Li, G., Liu, N., Wu, W., Pan, J., Chen, C., Jiao, Y., Deng, H., Ye, J., Zhang, X., Huang, H., Li, Q., Xue, L., Zhang, X., Tang, G., 2020. PLoS Biol. 18, e3000978.
Xiong, Y., Zhang, J., Yang, Z., Mou, Q., Ma, Y., Xiong, Y., Lu, Y., 2019. J. Am. Chem. Soc. 142, 207–213.
Yi, Z., de Dieu Habimana, J., Mukama, O., Li, Z., Odiwuor, N., Jing, H., Nie, C., Hu, M., Lin, Z., Wei, H., Zeng, L., 2022. Biosensors 12, 1.
Yuan, T., Mukama, O., Li, Z., Chen, W., Zhang, Y., de Dieu Habimana, J., Zhang, Y., Zeng, R., Nie, C., He, Z., Zeng, L., 2020. Analyst 145, 6388–6394.
Yun, C.S., Javier, A., Jennings, T., Fisher, M., Hira, S., Peterson, S., Hopkins, B., Reich, N. O., Strouse, G.F., 2005. J. Am. Chem. Soc. 127, 3115–3119.
Zhang, Y.-m., Zhang, Y., Xie, K., 2020. Mol. Breed. 40, 11.
Zhang, Y., Chen, M., Liu, C., Chen, J., Luo, X., Xue, Y., Liang, Q., Zhou, L., Tao, Y., Li, M., Wang, D., Zhou, J., Wang, J., 2021. Sensor. Actuator. B Chem. 345, 130411.